Stochastic Dynamics of Baroclinic Waves

BRIAN F. FARRELL

Department of Earth and Planetary Sciences, Harvard University, Cambridge, Massachusetts

PETROS J. IOANNOU

Center for Meteorology and Physical Oceanography, Massachusetts Institute of Technology, Cambridge, Massachusetts

(Manuscript received 8 January 1993, in final form 4 May 1993)

ABSTRACT

The maintenance of variance and attendant heat flux in linear, forced, dissipative baroclinic shear flows subject to stochastic excitation is examined. The baroclinic problem is intrinsically nonnormal and its stochastic dynamics is found to differ significantly from the more familiar stochastic dynamics of normal systems. When the shear is sufficiently great in comparison to dissipative effects, stochastic excitation supports highly enhanced variance levels in these nonnormal systems compared to variance levels supported by the same forcing and dissipation in related normal systems. The eddy variance and associated heat flux are found to arise in response to transient amplification of a subset of forcing functions that obtain energy from the mean flow and project this energy on a distinct subset of response functions (EOFs) that are in turn distinct from the set of normal modes of the system. A method for obtaining the dominant forcing and response functions as well as the distribution of heat flux for a given flow is described.

1. Introduction

The zonal wind in midlatitudes is to first approximation a jet in thermal wind balance with the temperature gradient maintained by differential insolation between the equator and pole. This jet is perturbed by synoptic-scale transient disturbances that are stochastically distributed in space and time and that have temperature and velocity variance generally increasing with the strength of the shear.

Various theories have been advanced to explain the origin and distribution of these transient cyclones and anticyclones. This interest can be traced in part to the influence of cyclones on weather: midlatitude weather forecasts are in good measure the predictions of cyclones and their tracks. But perhaps of equal importance is the contribution of the synoptic-scale transients to the long-term average transport of heat and momentum, which plays a central role in global climate.

A widely accepted explanation for the production and maintenance of transient perturbation variance in geophysical shear flows is that the undisturbed background state supports modal instability and that infinitesimal perturbations projecting on the unstable modes amplify exponentially through a sufficient number of e-foldings so that the instability becomes exponentially dominant over all other disturbances in the flow and eventually emerges as a modal wave of finite amplitude. Logical consequences of this paradigm include prediction of cyclogenesis based on the existence of local absolute instability (Pierrehumbert 1984; Lin and Pierrehumbert 1993), and adjustment of mean states by unstable waves to marginal stability configurations (Stone 1978; Lindzen and Farrell 1980; James 1987; Lindzen 1993). While modal instability theory has met with some success in model problems, it has not proven to be universally corroborated by observation.

An alternative viewpoint proceeds from the observation that although a given background flow may possess a large store of available energy and support a large perturbation variance under stochastic forcing, it need not as a necessary consequence support exponentially unstable modes (Farrell 1982, 1984, 1985, 1988, 1989b, 1990). Nonmodal growth of perturbations is required for explaining transition to turbulence in plane Couette and pipe Poiseuille flow, which support no unstable waves, and for plane Poiseuille flow which is observed to become turbulent at Reynolds numbers far below the critical value $R \approx 5772$ for which an instability of extremely small growth rate exists (Orszag 1971). It is suggested that this mechanism for transition is generally applicable and that maintenance of perturbation variance in a wide class of flows can be traced to amplification of nonmodal perturbations rather than to the growth of exponential modal instabilities (Farrell and Ioannou 1993b).

Corresponding author address: Dr. Brian F. Farrell, Dept. of Earth and Planetary Sciences, Harvard University, Pierce Hall, 29 Oxford St., Cambridge, MA 02138.

Consider a baroclinic jet maintained by strong thermal forcing so that while the background rate of strain field is modified by the perturbations, it is not to a first approximation determined by them. Certainly the initial growth of disturbances can be studied using linear theory and, if amplitudes remain sufficiently small, the maintenance of the perturbation field can also be studied using linear theory. In a forced/dissipative system with strong rates of strain but without exponential instability the flow behaves as an amplifier of perturbations (Farrell and Ioannou 1993a). At some high level of variance, nonlinear interactions will become important for providing the feedback perturbations required to sustain the variance and for limiting the potential amplification inherent in the linear problem. This central role of nonlinearity in the maintenance of fully developed turbulence is widely recognized, but perhaps less well recognized is the fact that the energetic exchange between the forced background flow and the perturbations arises solely from terms comprising the linear interaction between them (Joseph 1976).

In this work we determine the statistics of a stochastically excited pure baroclinic shear flow governed by linear dynamics. This model problem serves as an example of a larger class of dynamical systems that are governed by linearized dynamic equations and associated boundary conditions expressible in the form:

$$\frac{dx(t)}{dt} = \mathcal{A}x(t) + \xi(t), \tag{1.1}$$

where x is the vector field variable corresponding to the streamfunction collocated on points in directions of mean state variation; $\mathcal{A}$ is the operator of the linearized dynamics; and ξ represents the stochastic forcing (cf. Wang and Uhlenbeck 1945).

We assume that the linear operator $\mathcal{A}$ is time independent and asymptotically stable (i.e., all the eigenvalues of $\mathcal{A}$ that determine the asymptotic behavior of the dynamical system have negative real parts). The exclusive role of the linear terms in the energetics established by Joseph (1976) suggests a mean field approximation in which the background flow is taken as determined by factors exogenous to the perturbations under study, and the nonlinear terms describing the spectral transfer between perturbation scales is parameterized as a stochastic forcing. For simplicity, in the context of this mean field approximation we consider the deterministic background state to be time independent and the stochastic forcing to be white. Allowing time variation of the jet in (1.1), would result in a great increase in complexity. We consider the analysis of such nonautonomous stochastic dynamical systems an important and challenging problem for future work to be undertaken after the dynamics of the autonomous system is well understood.

The assumption that the linear dynamical operator is stable implies that the atmospheric statistics arise predominantly from nonmodal transient dynamics. This assumption does not preclude the interpretation that for an asymptotically unstable operator the nonlinear disruption of the motion would limit the duration of coherence, which could be incorporated in the linear dynamical operator by augmenting viscosity (Salmon 1980). The main difference from previous work (Salmon 1980; Haidvogel and Held 1980; Vallis 1988) is that we postulate that the maintenance of the atmospheric variance and the atmospheric energetics can be modeled as stochastic amplification of transient disturbances with appropriate parameterization of nonlinear effects. The linearization assumed here is similar to that assumed in the rapid distortion theory of turbulent flows (Townsend 1976; Hunt et al. 1991).

In general, solution of (1.1) requires numerical integration, although closed form solutions to the barotropic vorticity equation exist in the special case of unbounded constant shear and deformation (Moffat 1967; Boyd 1983; Tung 1983; Craik and Criminale 1986), allowing reduction of the stochastic excitation problem to a quadrature (Farrell and Ioannou 1993a).

As a familiar example of stochastic dynamics, consider white noise forcing of the damped harmonic oscillator equation that describes stochastic excitation of a unit mass spring or pendulum:

$$\frac{d^2x}{dt^2} + \gamma\frac{dx}{dt} + \omega_0^2 x = \xi(t), \tag{1.2}$$

where x is the displacement, γ the damping coefficient, ω_0^2 the restoring force linear in x, and $\xi(t)$ the forcing. Taking the Fourier transform pair:

$$x(t) = \int_{-\infty}^{\infty} \hat{x}(\omega)e^{i\omega t}d\omega \tag{1.3a}$$

$$\hat{x}(\omega) = \frac{1}{2\pi}\int_{-\infty}^{\infty} x(t)e^{-i\omega t}dt, \tag{1.3b}$$

the Fourier transform of (1.2) is

$$(-\omega^2 + i\gamma\omega + \omega_0^2)\hat{x}(\omega) = \hat{\xi}(\omega). \tag{1.4}$$

The ensemble average displacement is

$$\langle |x|^2 \rangle = \int_{-\infty}^{\infty}\int_{-\infty}^{\infty} \frac{\langle \hat{\xi}(\omega)\hat{\xi}^*(\omega')\rangle}{(\omega^2 - i\gamma\omega - \omega_0^2)(\omega'^2 + i\gamma\omega' - \omega_0^2)} \times e^{i(\omega-\omega')t}d\omega d\omega', \tag{1.5}$$

where $\langle\ \rangle$ represents the ensemble average and the star indicates complex conjugation. This response is influenced both by the spectral distribution of the driving through $\hat{\xi}(\omega)$ and the response of the system, which for small damping is peaked near ω_0. With white noise driving,

$$\langle \hat{\xi}(\omega)\hat{\xi}^*(\omega')\rangle = \frac{\dot{\xi}}{2\pi}\delta(\omega - \omega'),$$

the variance can be found by contour integration,

$$\langle |x|^2 \rangle = \frac{\dot{\xi}}{2\omega_0^2 \gamma}. \tag{1.6}$$

It is well known that coherent forcing of the undamped oscillator at its resonant frequency results in a harmonic displacement amplitude growing linearly with time and that off-resonance forcing results in a finite displacement amplitude. Remarkably, the response to incoherent forcing in the absence of damping is also unbounded; further analysis shows that in this case $\langle |x|^2 \rangle$ grows as t. Inspection of (1.6) reveals that the variance is also unbounded when the restoring force vanishes, regardless of the damping—this is Brownian motion, which is known to be nonstationary with $\langle |x|^2 \rangle$ also growing as t.

The harmonic oscillator example encompasses the physical process operating in linear normal dynamical systems for which the dynamical operator commutes with its Hermitian transpose. For normal dynamical systems resolution of the motion into its orthonormal modes allows each mode to be analyzed in isolation, and the total variance of the motion can be found by taking the sum of contributions from each of the individual normal modes. Furthermore, the variance contribution from each mode is inversely proportional to the damping rate of that mode. This can be understood as resulting from the amplitude of the response rising until the loss of energy to dissipation balances the input of energy from driving. The forcing is the only source of energy to the normal modes, and the energy associated with the variance is accumulated from this forcing, resulting, for a given forcing amplitude, in high variance only if damping is small.

Consider now a fluid with a background flow field having nonvanishing rate of strain but with sufficient dissipation so that all small perturbations impressed on the flow eventually decay. Linearization of the dynamical system about the background flow results in a nonnormal linear dynamical operator (i.e., the dynamical operator does not commute with its Hermitian transpose) and an associated set of modes that decay individually but that are not mutually orthogonal either in the inner product associated with the L_2 norm or in that associated with energy. This mathematical property of nonorthogonality of modes is indicative of an important physical property. The lack of mode orthogonality corresponds to the potential for extraction of energy by the perturbations from the background flow field despite the absence of exponential instability (Orr 1907; Farrell 1982). The energy balance in such a system is between the stochastic driving together with the induced extraction of energy from the background flow, on the one hand, and the dissipation on the other. Tapping the mean flow energy can lead to levels of variance orders of magnitude larger than would have been expected to result in a normal system from the rate of dissipation of each mode. Without stochastic driving the perturbation field vanishes. With stochastic forcing the level of variance in a nonnormal system may be maintained predominantly by the stochastically induced transfer of background flow energy to the perturbation field rather than by accumulation of energy from the forcing, as is the case for normal systems such as the harmonic oscillator.

Inspection of the observed global annual energy cycle provides an indication of the balances in this nonnormal dynamical system: the maintained energy is 18.4 $\times 10^5$ J m^{-2}, requiring a perturbation energy input of 0.7 W m^{-2} with transfer of energy from the mean to the eddies of the order of 1.27 W m^{-2}, and dissipation of 1.7 W m^{-2} (Oort and Peixoto 1983). The primary balance is between the transfer of energy from the mean and the dissipation, rather than between energy input and the dissipation as would occur for a normal dynamical system.

Recent theoretical and observational advances (Farrell 1985; Sanders 1986; Nordeng 1990) support a shift away from identification of flow disturbances with exponential modal instabilities toward recognition of the role of a wider subset of disturbances that contribute to the transient wave variance. From this perspective the nature of the imposed perturbation plays a central role. In an attempt to understand further the role of perturbations, this work explores the mechanism by which variance is maintained by stochastically inducing transfer of background flow energy to the variance field.

2. Formulation

We restrict attention to the linear dynamics of perturbations to a baroclinic mean state in a midlatitude β-plane channel the parameters of which vary only with height z in the domain $0 < z < z_t$, where z_t will be taken to correspond to an altitude of 40–80 km. The zonal direction, x, is taken to be unbounded and the meridional direction, y, is confined by channel walls to $-y_c \leq y \leq y_c$. The Coriolis parameter is taken as $f = f_0 + \beta y$. Variation of static stability modeling a stratosphere is included. We also consider vertical density variation with a constant scale height,

$$H = -\frac{1}{\rho}\frac{d\rho}{dz}.$$

For simplicity, following Charney (1947), we have adopted an independent specification of static stability and temperature. Such a specification allows a simple and realistic transition to stratospheric static stability, which although not strictly thermodynamically consistent is widely used as an approximation and introduces small errors.

With these assumptions the quasigeostrophic perturbation potential vorticity equation and boundary conditions with constant linear damping at the rate R

and Ekman damping with coefficient Γ_0 second in the scaled streamfunction:

$$\phi(z, t) = \psi(z, t) \frac{e^{z/2}}{\sqrt{\epsilon}} e^{ikx} \cos(ly), \quad (2.1)$$

takes the nondimensional form:

$$\left(\frac{\partial}{\partial t} + R + ikU\right)\left[\frac{\partial^2\psi}{\partial z^2} - \left(\frac{\alpha^2}{\epsilon} + S^2 - \frac{dS}{dz}\right)\psi\right] + ikQ_y\psi = 0, \quad (2.2.a)$$

$$\left(\frac{\partial}{\partial t} + R + ikU\right)\left(\frac{\partial\psi}{\partial z} + S\psi\right) - ik\left(\frac{dU}{dz} - \Gamma_0\right)\psi = 0, \quad z = 0, \quad (2.2.b)$$

$$\left(\frac{\partial}{\partial t} + R + ikU\right)\left(\frac{\partial\psi}{\partial z} + S\psi\right) - ik\frac{dU}{dz}\psi = 0, \quad z = z_t, \quad (2.2.c)$$

where time has been nondimensionalized by $1/f_0$, vertical distance by H, and horizontal distance by $H/\sqrt{\epsilon_0}$, where $\epsilon_0 = f_0^2/N_0^2$ is the square of the ratio of the Coriolis parameter to a characteristic Brunt–Väisälä frequency, and the total horizontal wavenumber is $\alpha = \sqrt{k^2 + l^2}$, so that the dimensional variables (denoted with a tilde) are

$$\tilde{t} = \frac{t}{f_0}$$
$$\tilde{\epsilon} = \epsilon_0\epsilon$$
$$\tilde{k} = \frac{\sqrt{\epsilon_0}k}{H}$$
$$\tilde{l} = \frac{\sqrt{\epsilon_0}l}{H}$$
$$\tilde{z} = Hz$$
$$\tilde{U} = \frac{f_0HU}{\sqrt{\epsilon_0}}$$
$$\tilde{\beta} = \frac{f_0\sqrt{\epsilon_0}\beta}{H}. \quad (2.3)$$

The problem is characterized by an Ekman parameter

$$\Gamma_0 = \frac{i}{H}\left(\frac{\nu}{2f_0}\right)^{1/2}\frac{\alpha^2}{\epsilon k}, \quad (2.4)$$

where ν is the coefficient of vertical eddy diffusion; a mean potential vorticity gradient,

$$Q_y = \frac{\beta}{\epsilon} + 2S\frac{dU}{dz} - \frac{d^2U}{dz^2}, \quad (2.5)$$

and a stability parameter

$$S = -\frac{1}{2}\left(\frac{1}{\epsilon}\frac{d}{dz}\epsilon - 1\right). \quad (2.6)$$

In (2.2) we have included damping arising from the vertical velocity induced by Ekman convergence at the ground and a constant linear damping at the rate R. The meridional dependence in (2.1) satisfies the boundary condition $\phi = 0$ at the channel walls, which are taken to broadly correspond to the latitudinal extent of the jet. The meridional wavenumber is related to the half-width of the jet, y_c, by $l = \pi/2y_c$.

The nonstandard nondimensionalization of time by the inverse of the Coriolis parameter was selected in order to retain the maximum zonal velocity of the background flow, which is more commonly employed in the nondimensionalization of time, as a free parameter. With the chosen nondimensionalization the maximum velocity becomes equal to the Rossby number, and consequently the nondimensional velocity needs to be chosen small compared to 1 to maintain the validity of the quasigeostrophic equations.

We choose values of the parameters appropriate for the midlatitude atmosphere: $f_0 = 10^{-4}\ \mathrm{s}^{-1}$, $N = 10^{-2}\ \mathrm{s}^{-1}$, $H = 10$ km, and $\tilde{\beta} = 1.6 \times 10^{-11}\ \mathrm{m}^{-1}\ \mathrm{s}^{-1}$. This results in $\beta = 0.16$, a horizontal wavenumber $k = 1$ corresponding to 1550 km, and a unit of nondimensional time corresponding to $2.8h$. We will consider linear damping with $R = 0.01$ giving a dimensional e-folding interval of 11.5 days. The value of the Ekman parameter over a neutrally stratified oceanic boundary layer corresponds to a coefficient of vertical diffusion ν of about $5\ \mathrm{m}^2\ \mathrm{s}^{-1}$, while over flat land with neutral stratification the appropriate value of ν is appreciably higher, typically $50\ \mathrm{m}^2\ \mathrm{s}^{-1}$ [Ekman damping parameterizations derived from the boundary-layer model employed by ECMWF are discussed in Lin and Pierrehumbert (1988); see also Gill (1982)]. We will consider eddy viscosity $\nu = 10\ \mathrm{m}^2\ \mathrm{s}^{-1}$, unless otherwise stated. This leads to an Ekman number $E_V = H^{-1}\sqrt{\nu/2f_0} = 0.0225$.

The zonal wind is chosen to be

$$U = sz - [sz - s(z - z_0)]\frac{1 + \tanh[(z - z_0)/\delta]}{2} + s(z - z_0)\frac{1 + \tanh[(z - 2z_0)/\delta]}{2}, \quad (2.7)$$

with the zonal jet maximum occurring at nondimensional height $z_0 = 1.5$. The vertical extent of the atmospheric jet is controlled by δ, which we set equal to 0.15 nondimensional units. The parameter s is a nondimensional shear parameter, which will be varied. A zonal wind maximum at the tropopause of $45\ \mathrm{m\ s}^{-1}$ corresponds to $s = 0.3$. A typical variation of the mean zonal wind with height is shown in Fig. 1.

The stratification parameter, which with our nondimensionalization is related to the inverse square of the Brunt–Väisälä frequency, is taken to be of the form

$$\epsilon = \left[1 + 3\,\frac{1 + \tanh[(z - z_s)/\delta_s]}{2}\right]^{-1} \tag{2.8}$$

in order to simulate the increased stability in the stratosphere. The tropopause is located at $z_s = z_0 + \delta$, where z_0 is the height of the jet maximum, and the vertical extent of the transition to stratospheric values is controlled by $\delta_s = \delta/2$. The variation of ϵ with height is also shown in Fig. 1.

The dynamical system (2.1) for the variable $\hat{\phi}(z, t) = \epsilon^{-1/2} e^{z/2} \hat{\psi}(z, t)$ is written in operator form as

$$\frac{d\hat{\phi}}{dt} = \mathcal{B}\hat{\phi}, \tag{2.9}$$

where

$$\mathcal{B} \equiv \frac{e^{z/2}}{\sqrt{\epsilon}} (\Delta^{-1}(-ikU - R)\Delta - ik\Delta^{-1}Q_y) \frac{\sqrt{\epsilon}}{e^{z/2}}, \tag{2.10.a}$$

with

$$\Delta \equiv \frac{\partial^2}{\partial z^2} - \left(\frac{\alpha^2}{\epsilon} + S^2 - \frac{dS}{dz}\right), \tag{2.10.b}$$

and Δ^{-1} rendered unique with the incorporation of boundary conditions (2.2.b,c). The dynamical system (2.9) is solved for $\hat{\phi}(z, t)$ given an initial state $\hat{\phi}_0$ specified at $t = 0$.

Consider the finite-difference approximation to (2.10.a,b). The generalized coordinate for an N-level discretization is a vector,

$$\hat{\phi}(t) = \begin{bmatrix} \hat{\phi}_1 \\ \vdots \\ \hat{\phi}_i \\ \vdots \\ \hat{\phi}_N \end{bmatrix}, \tag{2.11}$$

where $\hat{\phi}_i$ is the value of the variable at the ith discretized level, z_i, and $\mathcal{B}$ becomes an $N \times N$ complex matrix. By this means, the continuous dynamical system (2.9) is approximated as a finite dimensional dynamical system. Reduction of the continuous dynamical system to a finite dimensional system is central to current methods of modeling atmospheric dynamics. Correspondence between the continuous and discrete dynamical system is assumed in numerical weather prediction models, where typically a relatively small number of vertical levels are employed. We note the tenuousness of this correspondence, to which we will return in the discussion, and employ a large number of discretization levels (typically 200 levels), which we double to verify convergence.

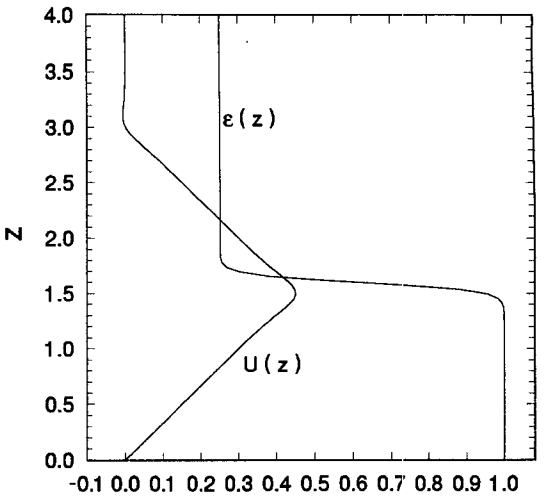

FIG. 1. The nondimensional mean flow velocity and Brunt–Väisälä frequency variation with height. The nondimensional shear is $s = 0.3$ corresponding to a dimensional maximum zonal velocity of 45 m s^{-1}, and $\epsilon = 1$ in the troposphere corresponds to Brunt–Väisälä frequency $N = 10^{-2}$ s^{-1}.

Returning to the formulation of the discretized problem, the perturbation energy is defined at time, t, as

$$E^t(k, l) = \frac{1}{8}\int_0^{z_t} dz\rho\left(\alpha^2\hat{\phi}^*\hat{\phi} + \epsilon\frac{\partial\hat{\phi}^*}{\partial z}\frac{\partial\hat{\phi}}{\partial z}\right) \tag{2.12.a}$$

$$= \hat{\phi}^\dagger(t)\mathcal{M}\hat{\phi}(t), \tag{2.12.b}$$

in which $\hat{\phi}^\dagger$ is the Hermitian transpose of $\hat{\phi}$ and the energy metric, $\mathcal{M}$, is given by

$$\mathcal{M} = -\frac{\delta}{8}[(\mathcal{E}\mathcal{D})^\dagger\mathcal{E}\mathcal{D} + \alpha^2\mathcal{P}^2], \tag{2.13}$$

with δ the grid size, $\mathcal{D}$ the discretized first-order d/dz operator, $\mathcal{P}^2_{ij} \equiv \rho(z_i)\delta_{ij}$, and $\mathcal{E}_{ij} \equiv \sqrt{\rho(z_i)\epsilon(z_i)}\,\delta_{ij}$ (δ_{ij} the Kronecker delta).

3. Stochastic excitation of perturbation variance

We wish to determine the statistical evolution of the perturbation energy density, E, under stochastic forcing. It is advantageous to transform the dynamical equation (2.9) into generalized velocity variables $u = \mathcal{M}^{1/2}\hat{\phi}$. The quasigeostrophic dynamic equation in this variable takes the form:

$$\frac{du_i}{dt} = \mathcal{A}_{ij}u_j + \mathcal{F}_{ij}\xi_j, \tag{3.1}$$

where

$$\mathcal{A} = \mathcal{M}^{1/2}\mathcal{B}\mathcal{M}^{-1/2}, \tag{3.2}$$

and ξ is the random forcing assumed to be a δ-correlated Gaussian white noise process with zero mean: $\langle \xi_i \rangle = 0, \langle \xi_i(t)\xi_j^*(t') \rangle = \dot{\xi}_i \delta_{ij} \delta(t - t')$, which excites independently each spatial forcing distribution specified by the columns $f^{(j)}$ of the matrix $\mathcal{F}_{ij}$. Unless otherwise indicated, all $\dot{\xi}_i$ will be taken of equal magnitude $\dot{\xi}$ which, by scaling the forcing matrix $\mathcal{F}$, can be taken equal to unity. We want to determine the evolution of the variance sustained by (3.1), which in physical variables is the ensemble-averaged energy density $\langle E^t \rangle = \langle u_i^*(t) u_i(t) \rangle$, and its limit $\langle E^\infty \rangle = \lim_{t->\infty} \langle u_i^*(t) u_i(t) \rangle$, when this limit exists.

Note that the operator $\mathcal{A}$ is in general nonnormal; that is, $\mathcal{A}^\dagger \mathcal{A} \neq \mathcal{A}\mathcal{A}^\dagger$ ($\dagger$ denotes the Hermitian transpose) so that the eigenvectors of $\mathcal{A}$ are not necessarily orthogonal and transient growth not associated with modal instability is possible. Nonnormality of $\mathcal{A}$ stems from the fact that the underlying dynamical system is not energetically closed so that the mean flow and the perturbations can exchange energy. If $\mathcal{A}$ is normal, as is the case in the absence of basic-state shear, transformation into normal coordinates yields directly the generalization of (1.6): the level of variance is then the sum of the variance in each of the normal coordinates forced independently (Wang and Uhlenbeck 1945). Thus,

$$\langle E^t_{\text{herm}} \rangle = \sum_{i=1}^{N} -\frac{\dot{\xi}_i}{2\sigma_i} [1 - \exp(2\sigma_i t)], \quad (3.3)$$

where $\dot{\xi}_i$ is the magnitude of forcing of the ith eigenfunction of the normal operator $\mathcal{A}$ and σ_i is the corresponding eigenvalue. When the eigenvalues are negative, as is the case for asymptotically stable dynamics, the variance approaches a statistically steady value at which the accumulated energy produces a balance between the rate of energy injection and the rate of energy dissipation and in which the maintained variance is proportional to a weighted sum of the inverse of the decay rate of its modes. Due to energy exchange with the mean, nonnormal dynamical systems do not allow such a straightforward characterization, and a generalized calculus for determining the evolution of the ensemble average variance is needed (cf. Ioannou 1992; Farrell and Ioannou 1993b).

Before embarking on a calculation of the ensemble average energy density we return to the issue of correspondence between the discrete and continuous system. The variance of the continuous system is found by infinite summations of the form (3.3) and questions of convergence as a function of N naturally arise. Related to this is the convergence as $N \to \infty$ of the energy input $\sum_{i=1}^{N} \dot{\xi}_i$. Consequently, we seek the factor by which the energy density of the response exceeds the energy density input over unit time:

$$G = \lim_{N\to\infty} \frac{\langle E^t \rangle}{\sum_{i=1}^{N} \dot{\xi}_i}, \quad (3.4)$$

where here $\dot{\xi}_i$ is the energy input over unit time to the ith forcing function.

Convergence of (3.4) will depend on the form of dissipation included in the dynamical operator $\mathcal{A}$. In laboratory flows governed by the Navier–Stokes equations, molecular diffusion strongly dissipates the more highly structured vertical modes of the system and $\langle E^t \rangle$ is rapidly convergent. However, the total energy input diverges as $N \to \infty$ unless the forcing distribution is tapered off at higher mode number to render the energy input finite. A natural choice for such a rolloff of the forcing at high mode number is the distribution characteristic of fully developed homogeneous turbulence (Farrell and Ioannou 1993b). In contrast, quasigeostrophic dynamics with linear damping does not selectively damp higher-order vertical modes, and this leads to divergence of $\langle E^t \rangle$ as $N \to \infty$. In that case and in the absence of tapering of the forcing, (3.4) is an indefinite form, although it may have a limit associated with a divergent input of energy. Correspondence with the continuous system can be obtained either by including vertical diffusion in the quasigeostrophic formulation or by limiting the forcing to a restricted pass band. In this work we have selected the second alternative. In calculating the variance we will make the assumption that the stochastic forcing is limited to the first 25 vertical wavenumbers in the troposphere. Under this assumption both the variance, $\langle E^t \rangle$, and the amplification factor, G, of the discretized system converge as the number of discretization levels increases.

We return now to the dynamical system (3.1), the solution of which, for $t \geq 0$ with initial condition u_0, is given by

$$u = e^{\mathcal{A}t} u_0 + \int_0^t \mathcal{G}(t - s) \mathcal{F} \xi ds, \quad (3.5)$$

where $\mathcal{G}(t - s) = e^{\mathcal{A}(t-s)}$. The random response, u, is linearly dependent on ξ and consequently is also Gaussian distributed. The first moment, given by $\langle u \rangle = e^{\mathcal{A}t} u_0$, vanishes for large times if we assume that $\mathcal{A}$ is stable, in which circumstance the statistics are independent of the initial conditions, which will henceforth be taken to be zero. The temporal development of the variance due to forcing initiated at $t = 0$ is given by

$$\begin{aligned} \langle E^t \rangle &= \langle u_i^*(t) u_i(t) \rangle \\ &= \mathcal{F}^*_{lb} \left(\int_0^t \mathcal{G}^*_{ba}(t - s) \mathcal{G}_{ad}(t - s) ds \right) \mathcal{F}_{dl} \\ &= \sum_l f_b^{*(l)} \mathcal{H}^t_{ba} f_a^{(l)}. \end{aligned} \quad (3.6)$$

We have defined $\mathcal{H}^t \equiv \int_0^t \mathcal{G}^\dagger(t - s) \mathcal{G}(t - s) ds$, and $f_a^{(b)} \equiv \mathcal{F}_{ab}$. Recall that $f_a^{(b)}$ represents the ath coordinate of the bth forcing function.

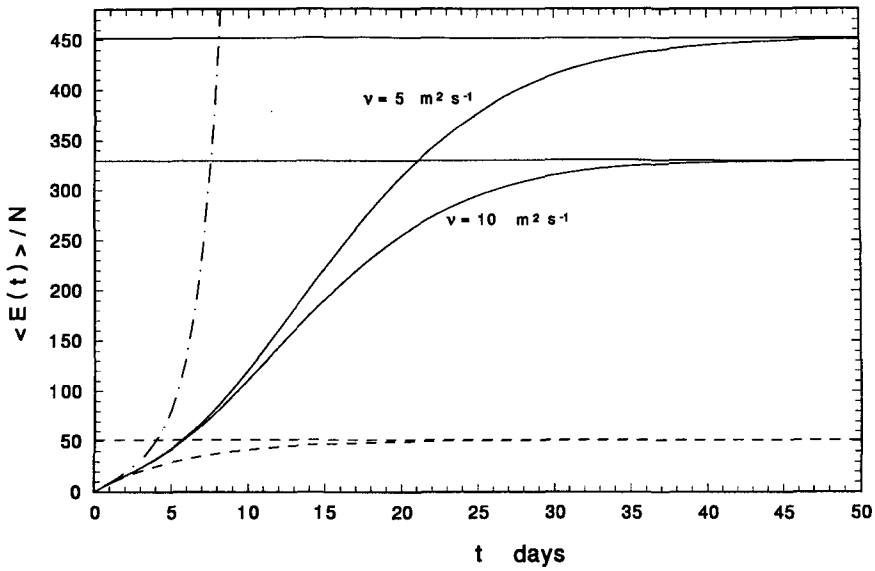

FIG. 2. Time development of the ensemble average energy density amplification, $\langle E \rangle / N$. For this integration $N = 200$ and all degrees of freedom are equally forced. The baroclinic basic state has shear $s = 0.3$, corresponding to a maximum jet speed at the tropopause of 45 m s^{-1}. The rate of linear damping is $R = 0.01$. The wave with $k = 2$, $l = 2$ is shown for eddy diffusion coefficient $\nu = 5$ m^2 s^{-1} and $\nu = 10$ m^2 s^{-1}. The dashed curve shows the evolution of the variance as it would occur if the dynamical system were normal with $\nu = 10$ m^2 s^{-1}. The dash–dot curve shows the evolution of the variance according to linear dynamics with $\nu = 0$ and $R = 0$, in which case the dynamical system is asymptotically unstable.

The evolution equation for $\mathcal{K}^t$ with initial condition $\mathcal{K}^0 = 0$ can be derived by direct time differentiation of $\mathcal{K}^t$. It is

$$\frac{d}{dt}\mathcal{K}^t = \mathcal{I} + \mathcal{A}^\dagger \mathcal{K}^t + \mathcal{K}^t \mathcal{A}, \tag{3.7}$$

in which $\mathcal{I}$ is the identity matrix. The asymptotic stability of $\mathcal{A}$ ensures the existence of $\mathcal{K}^\infty = \lim_{t\to\infty} \mathcal{K}^t$ and therefore of the statistical steady-state response to stochastic forcing. The asymptotic value can be determined from the Lyapunov equation:

$$\mathcal{A}^\dagger \mathcal{K}^\infty + \mathcal{K}^\infty \mathcal{A} = -\mathcal{I}, \tag{3.8}$$

which can be solved by standard methods (Lefschetz 1963).

It can be readily verified that the solution to (3.7) is

$$\mathcal{K}^t = \mathcal{K}^\infty - e^{\mathcal{A}^\dagger t} \mathcal{K}^\infty e^{\mathcal{A} t}. \tag{3.9}$$

Note that when $\mathcal{A}$ is not asymptotically stable, $\mathcal{K}^\infty$ diverges according to the linear approximation of the dynamics, but that the time development of the variance can still be obtained by direct numerical integration of (3.7).

The variance arising from stochastic forcing alone is

$$\langle E^t \rangle = \text{trace}(\mathcal{F}^\dagger \mathcal{K}^t \mathcal{F}) = \text{trace}(\mathcal{F}\mathcal{F}^\dagger \mathcal{K}^t). \tag{3.10}$$

With a complete orthogonal set of forcing functions so that $\mathcal{F}\mathcal{F}^\dagger = \mathcal{I}$, the expression for the energy density simplifies to $\langle E^t \rangle = \text{trace}(\mathcal{K}^t)$ and the variance is independent of the specific forcing distribution; that is, any full rank unitary forcing distribution will lead to the same variance. This result is not true for weighted forcing distributions. In Fig. 2 we show the approach of $\langle E^t \rangle$ to its asymptotic value. For comparison and to make contact with a normal system, we have also included in the same graph the evolution of the variance as it would have occurred if each of the modes were contributing to the variance according to the mode decay rate as in (3.3), interpreting in this way $\mathcal{A}$ as a normal operator. Note the reduced level of variance. In general we find, for atmospheric values of parameters, that the associated normal system supports levels of variance that are typically an order of magnitude smaller than are supported by the actual nonnormal dynamical system. The increase of the variance with the degree of nonnormality, which varies with the shear of the background flow, is shown by a plot of the variance sustained as a function of shear in Fig. 3. The time development of variance in the absence of dissipation is also shown in Fig. 2. In this case $\mathcal{A}$ is unstable and linear theory eventually becomes inadequate.

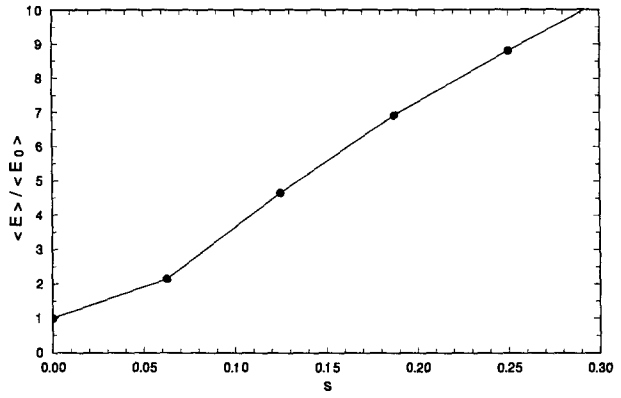

FIG. 3. Variation of ensemble average energy as a function of shear s. The variance has been normalized by its value $\langle E_0 \rangle$ at zero shear in which case the dynamical operator $\mathcal{A}$ is normal. A shear typical of the storm track would be $s = 0.3$. In this calculation, we have assumed that the random forcing is limited to vertical wavenumber 25 in the troposphere.

An illustrative alternative to the time-domain analysis employed above is to obtain the asymptotic ensemble energy density $\langle E^\infty \rangle$ from the frequency response of the dynamical system following the method presented in section 1 for the harmonic oscillator. Fourier transformation of (3.1) readily yields that

$$\langle E^\infty \rangle = \frac{\dot{\xi}}{2\pi} \int_{-\infty}^{\infty} F(\omega) d\omega, \tag{3.11}$$

where the energy weighted frequency response,

$$F(\omega) = \text{trace}(\mathcal{R}^\dagger(\omega)\mathcal{R}(\omega)), \tag{3.12a}$$

is obtained from the resolvent

$$\mathcal{R}(\omega) = (i\omega\mathcal{I} - \mathcal{A})^{-1}. \tag{3.12b}$$

Note that mode coupling due to the nonnormality of the operator $\mathcal{A}$ leads to an energy response function $F(\omega)$ that cannot be simply characterized as a summation of contributions from the poles of the resolvent. This alternative method of determining the asymptotic variance is informative because it reveals the frequency distribution of contributions to the variance, but it is numerically inefficient compared to the previous method that relies on solution of the Lyapunov equation. In Fig. 4 the response function for a perturbation with $k = 2$, $l = 2$ and shear $s = 0.3$ in basic state (2.7) is shown. The main contribution to the variance arises from frequencies producing phase speeds contained within the flow; that is, $0 \leq \omega/k \leq U_{\max}$ (for the case shown $U_{\max} = 0.45$). The frequency decomposition of the ensemble average energy is concentrated in the low-frequency domain (i.e., it has a red spectrum) and possesses two maxima associated with distinct surface and tropopause disturbances, which for this 45 m s^{-1} jet have approximate periods of 4.5 days and 1 day, respectively, with corresponding phase speeds of 8 m s^{-1} and 35 m s^{-1}. In formulating the stochastic excitation we have assumed that the random forcing is white. However, the quasigeostrophic dynamics itself implies that the dominant response of the baroclinic atmosphere is concentrated in periods longer than a day. The high-frequency components of the forcing spectrum do not lead to a significant response. If we had used a red forcing spectrum, we would expect an even more enhanced redness of the response.

The fields resulting from (3.1) are Gaussian with zero mean. Their statistical specification can be obtained from the correlation matrix, taking into account the assumed δ correlation of ξ:

$$\begin{aligned} \mathcal{C}^t_{ij} &= \langle u_i(t) u_j^*(t) \rangle \\ &= \left\langle \int_0^t ds \int_0^t ds' \mathcal{G}_{ib}(t-s)\mathcal{F}_{bc}\xi_c(s) \right. \\ &\qquad \left. \times \mathcal{G}^*_{je}(t-s')\mathcal{F}^*_{eg}\xi^*_g(s') \right\rangle \qquad (3.13) \\ &= \int_0^t ds \mathcal{G}_{ib}(t-s)\mathcal{F}_{bc}\mathcal{F}^*_{ec}\mathcal{G}^*_{je}(t-s) \\ &= \int_0^t ds \mathcal{G}_{ib}(t-s)\mathcal{F}_{bc}\mathcal{F}^\dagger_{ce}\mathcal{G}^\dagger_{ej}(t-s), \end{aligned}$$

or in matrix form

$$\mathcal{C}^t = \int_0^t \mathcal{G}(t-s)\mathcal{G}^\dagger(t-s) ds, \tag{3.14}$$

in which forcing distributions are assumed to satisfy: $\mathcal{I} = \mathcal{F}\mathcal{F}^\dagger$.

Clearly $\mathcal{C}^0 = 0$ and, due to the asymptotic stability of $\mathcal{A}$, stationary statistics are achieved so that $\lim_{t\to\infty} \mathcal{C}^t = \mathcal{C}^\infty$. The evolution equation of the correlation matrix is

$$\frac{d}{dt}\mathcal{C}^t = \mathcal{I} + \mathcal{A}\mathcal{C}^t + \mathcal{C}^t\mathcal{A}^\dagger. \tag{3.15}$$

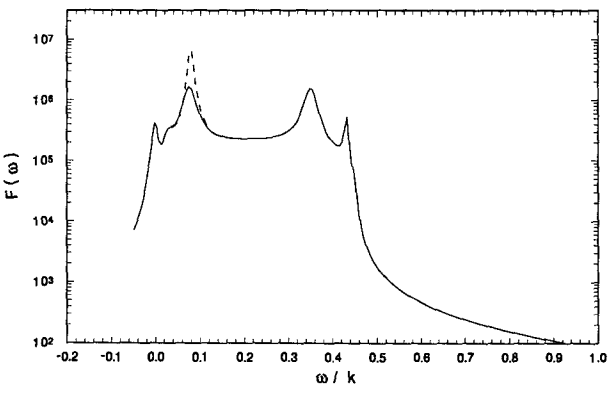

FIG. 4. The energy frequency response function $F(\omega)$ of the baroclinic atmosphere. The mean state is as in Fig. 3 with $k = 2$, $l = 2$. The responses for $\nu = 10$ m^2 s^{-1} (solid) and for $\nu = 5$ m^2 s^{-1} (dots) are shown.

To obtain the asymptotic value of the correlation matrix, we proceed as in (3.8) to solve the associated Lyapunov equation:

$$\mathcal{A}\mathcal{C}^{\infty} + \mathcal{C}^{\infty}\mathcal{A}^{\dagger} = -\mathcal{I}, \tag{3.16}$$

which determines the time evolution of the correlation matrix as

$$\mathcal{C}^{t} = \mathcal{C}^{\infty} - e^{\mathcal{A}t}\mathcal{C}^{\infty}e^{\mathcal{A}^{\dagger}t}. \tag{3.17}$$

Note that, due to the nonnormality of $\mathcal{A}$, expressions (3.16) and (3.17) are not the Hermitian conjugates of (3.7) and (3.8). This has the physical significance, as will be explained in the sequel, that $\mathcal{H}^{t}$ is associated with the structures forcing the variance, while $\mathcal{C}^{t}$ is associated with the structures of the resulting response.

The correlation matrix is a positive definite Hermitian operator by construction, and therefore it has real and positive eigenvalues associated with mutually orthogonal eigenvectors. Each eigenvalue equals the variance accounted for by the pattern of its corresponding eigenvector. The decomposition of the correlation matrix into its orthogonal components is called the EOF decomposition (Lorenz 1956). To determine the EOF decomposition we solve the eigenvalue problem:

$$\mathcal{C}^{\infty}u^{(i)} = \lambda^{(i)}u^{(i)}. \tag{3.18}$$

In the energy norm the EOFs determine an orthogonal set of generalized velocity response functions, with corresponding streamfunctions given by $\hat{\phi} = \mathcal{M}^{-1/2}u$, which can be ordered by their contribution to the variance using the eigenvalues $\lambda^{(i)}$. Note that, in contrast to the orthogonality of the underlying generalized velocities, these streamfunctions are not orthogonal.

We can proceed similarly to determine the eigenfunctions, $f^{(i)}$, of $\mathcal{H}^{\infty}$:

$$\mathcal{H}^{\infty}f^{(i)} = \mu^{(i)}f^{(i)}. \tag{3.19}$$

As can be verified by inspection of (3.6), these eigenfunctions determine the forcing distributions $f^{(i)}$ that render the functional

$$I[f] = \frac{f^{\dagger}\mathcal{H}^{\infty}f}{f^{\dagger}f} \tag{3.20}$$

stationary (note again that $\mathcal{H}^{\infty}$ is Hermitian and positive definite). The eigenfunctions $\phi^{i} = \mathcal{M}^{-1/2}f^{i}$ can be ordered according to their contribution to the maintained variance using the eigenvalues $\mu^{(i)}$.

We have determined and ordered two sets of orthogonal functions: using (3.19) we ordered the forcings according to their contribution to the variance, and using (3.18) we ordered the responses according to their contribution to the statistical steady-state correlation matrix. When $\mathcal{A}$ is normal, these two sets of orthogonal functions reduce to the eigenfunctions of $\mathcal{A}$ because $\mathcal{A}$, $\mathcal{H}^{t}$, and $\mathcal{C}^{t}$ commute and therefore are simultaneously diagonalizable by the same eigenvectors. For a normal operator the EOF patterns of the system response ordered according to their contribution to the variance are also the forcing modes of the system when they are also ordered according to their contribution to the variance, and these are both identical to the normal modes of $\mathcal{A}$. None of these three sets of functions is the same when $\mathcal{A}$ is nonnormal, as can be directly seen in Figs. 5a,b,c. Note that the first EOF (Fig. 5a) gives a realistic distribution of the eddy energy (cf. Fig. 26 of Oort and Peixoto 1983). North (1984) realized that when the operator is nonnormal, the EOF decomposition of the correlation matrix cannot be used to identify the dynamical modes of the system. For nonnormal systems, identification of those forcings responsible for the largest contribution to the variance of the statistical steady state becomes an important theoretical question, and we have found that these forcings can be identified by eigenanalysis of the matrix $\mathcal{H}^{\infty}$, which is obtained as the solution of the back Lyapunov equation (3.8); we call this ordered set of forcings the back EOF decomposition. In choosing a basis set for a complete dynamical investigation of a system, it is necessary to resolve both the subspace of the back EOF decomposition as well as that of the EOF decomposition because the former span the forcings that grow into the responses spanned by the latter.

4. Fluxes and energetics

The perturbation energy equation is derived in the usual way by multiplying (3.1) by the Hermitian conjugate of the generalized velocity, $u^{\dagger}$, and similarly multiplying by the generalized velocity the Hermitian conjugate of (3.1) and adding to obtain the ensemble average energy equation:

$$\frac{d}{dt}E^{t} = \langle u_i^{*}(\mathcal{A}_{ij}^{\dagger} + \mathcal{A}_{ij})u_j\rangle + \langle u_i^{*}\mathcal{F}_{ij}\xi_j + \xi_j^{*}\mathcal{F}_{ji}^{\dagger}u_i\rangle, \tag{4.1}$$

where $E^{t} = \langle u_i^{*}u_i\rangle$. Disregarding the transient solution of (3.5), we obtain

$$\langle u_i^{*}\mathcal{F}_{ij}\xi_j\rangle = \frac{N\dot{\xi}}{2}, \tag{4.2}$$

where N is the number of discretization levels. Assuming $\mathcal{A}$ is asymptotically stable, (4.1) becomes

$$\lim_{t\to\infty} -\langle u_i^{*}(\mathcal{A}_{ij}^{\dagger} + \mathcal{A}_{ij})u_j\rangle = N\dot{\xi}. \tag{4.3}$$

In the absence of shear, $\mathcal{A}$ is normal and (4.3) is a statement of balance between the rate of energy input and the rate of energy dissipation. In the presence of shear $\mathcal{A}$ is nonnormal and the lhs of (4.3) includes the additional term representing energy interaction with the basic flow. Note that in this case the spec-

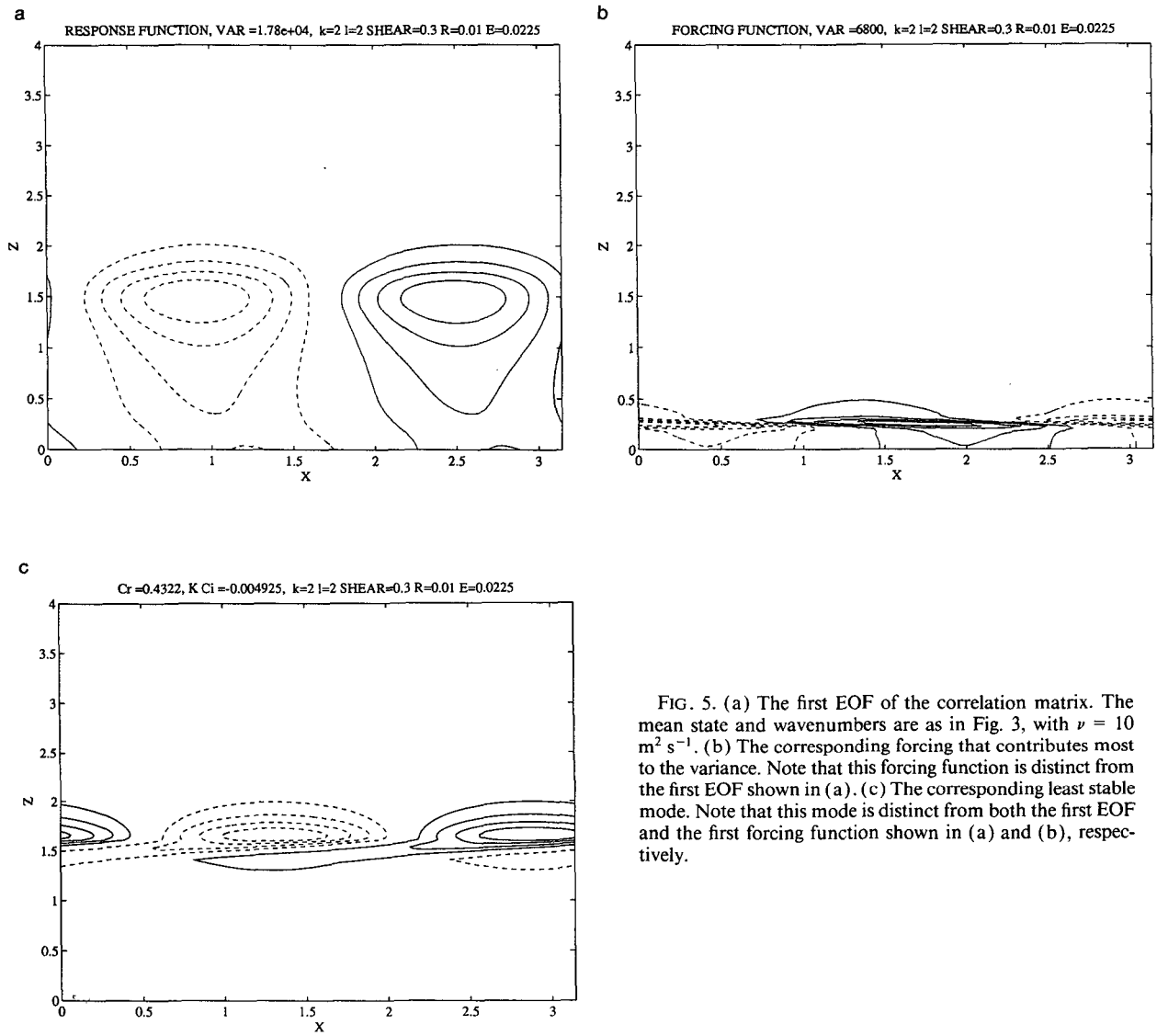

FIG. 5. (a) The first EOF of the correlation matrix. The mean state and wavenumbers are as in Fig. 3, with $\nu = 10$ $m^2 s^{-1}$. (b) The corresponding forcing that contributes most to the variance. Note that this forcing function is distinct from the first EOF shown in (a). (c) The corresponding least stable mode. Note that this mode is distinct from both the first EOF and the first forcing function shown in (a) and (b), respectively.

trum of $\mathcal{A}$ is different from the spectrum of $\mathcal{A} + \mathcal{A}^\dagger$ [which can be seen from inspection of the first term on the rhs of (4.1) to determine the initial growth of a disturbance]. This instantaneous rate of growth may be large despite the fact that asymptotically the disturbance must decay at a rate determined by the real part of the spectrum of $\mathcal{A}$, which may be strongly damped. This initial growth arising from the existence of positive eigenvalues of $\mathcal{A} + \mathcal{A}^\dagger$ implies energy exchange with the mean flow even when the spectrum of $\mathcal{A}$ is stable.

In unbounded shear flows, which support no modes, Farrell and Ioannou (1993a) found that, except for very small shears, fluxes are upgradient regardless of the dissipation, and the forcing serves ultimately to reinforce the mean shear. On the other hand, with the inclusion of a parameterization of the occlusion process that modeled the existence of modal solutions, the fluxes were found to be always downgradient. In the baroclinic problem, which supports damped modal solutions, we also find that the fluxes are downgradient for all shears and dissipations, a result consistent with the parameterized role of modes in the unbounded shear problem.

In order to identify terms in the energy equation responsible for energy exchange with the mean flow, we form the ensemble average perturbation energy density equation. Following the usual steps (cf. Lindzen 1990), we have in nondimensional variables:

$$\frac{d}{dt}\langle E^t\rangle = \int_0^\infty dz\langle \rho\epsilon U_z\overline{\phi_x\phi_z}\rangle - \int_0^\infty dz\langle \rho R\overline{(\phi_x^2+\phi_y^2+\epsilon\phi_z^2)}\rangle$$

$$- E_V\langle \rho\epsilon\overline{(\phi_x^2+\phi_y^2)}\rangle|_{z=0} + \int_0^\infty dz\langle \rho\overline{\phi F_{\text{noise}}}\rangle, \quad (4.4)$$

where the energy density E^t is given in (2.12), and the overbar signifies an average over the horizontal domain bounded in the meridional direction by the channel walls and one wavelength in the longitudinal direction. The term responsible for energy growth is the heat flux proportional to

$$H = \frac{k}{2}\rho\left\langle \text{Im}\left(\hat{\phi}^*\frac{\partial}{\partial z}\hat{\phi}\right)\right\rangle. \quad (4.5)$$

The heat flux can be calculated as the trace of the correlation matrix:

$$\mathscr{H}^t_{ij} = \frac{k}{2}\text{Im}(\langle \mathcal{P}_{ia}\mathcal{D}_{ab}\hat{\phi}_b\mathcal{P}_{jc}\hat{\phi}_c^*\rangle), \quad (4.6)$$

where $\mathcal{D}$ is the discretized d/dz operator and $\mathcal{P}_{ij} \equiv \sqrt{\rho(z_i)}\,\delta_{ij}$. Expression (4.6) reduces to

$$\mathscr{H}^t = \frac{k}{2}\text{Im}(\mathcal{P}\mathcal{D}\mathcal{M}^{-1/2}\mathscr{C}^t\mathcal{M}^{-1/2}\mathcal{P}), \quad (4.7)$$

where $\mathscr{C}^t$ is the correlation matrix given in (3.12). The correlation matrix of the generalized velocities determines the heat flux matrix and, in particular, the diagonal elements of $\mathscr{H}^t$ give the height distribution of the heat flux, an interesting property that may be of value in observational studies. An example of the distribution of the ensemble average heat flux is shown in Fig. 6. Note the second maximum near the tropopause, above which there is a southward heat flux in the stratosphere. Despite the southward flux in the stratosphere, the vertically integrated heat flux is positive. The realism of this distribution of the ensemble average heat flux can be immediately assessed by comparison with observations that are plotted in Fig. 7.

5. Discussion

In the inviscid baroclinic problem it is often found that the most unstable modal streamfunctions can be resolved with a limited number of vertical levels because modal solutions tend to have rather smooth vertical structure when damping is small, as in the familiar Charney and Eady problems. However, it has also been observed that very high levels of discretization are required to resolve nearly neutral small-scale waves (Green 1960; Bell and White 1988).

Inclusion of Ekman damping presents additional problems of correspondence between the continuous and discrete system; for example, it is known that Ekman damped discrete systems may support spurious numerical instabilities regardless of the level of discretization (Farrell 1989a). These instabilities occur because in the continuous system the phase speed of the unstable mode remains within the flow, while the growth rate decreases with increasing Ekman damping until a critical Ekman damping is reached for which the mode becomes neutral and above which the mode ceases to exist (Lin and Pierrehumbert 1988). The discrete system cannot capture the disappearance of the unstable mode with increasing Ekman damping when the critical level remains within the flow, but instead produces a spurious unstable mode. Inclusion of linear damping does not remove this spurious mode but does minimize its effects by causing it to decay.

Inspection of the first back EOF in Fig. 5b indicates that resolving the forcing functions in the stochastic problem also requires very high levels of discretization for realistic values of dissipation; typically $N = 200$ is needed for the examples in this work. It is difficult to escape the conclusion that modeling accurately the stochastic dynamics of the atmosphere requires these high resolutions.

It should also be noted that the vertical scale of the random forcing has an important impact on the maintained variance. For example, if we consider that forcing is restricted to the troposphere and required to have a low vertical wavenumber (as is the case in latent heat parameterizations in large model studies), then the projection of the forcing on the dominant back EOFs is reduced and this leads to a reduction of the sustained variance. This can be seen in Fig. 8, where we have chosen various minimum vertical scales of the stochastic forcing and calculated the sustained variance as a function of the shear. The zonal flows with higher shear have dominant back EOFs involving smaller scales and the projection of the stochastic forcing is increasingly ineffective, leading to saturation and even reduction of the variance with increasing shear (assuming exponential stability of the linear operator is maintained).

We turn now to the question of picking a metric by which to measure perturbation magnitude. Consider the norm generated by the full rank Hermitian matrix $\mathcal{M}$, for which $u = \mathcal{M}^{1/2}\hat{\phi}$ is the associated generalized variable. This generalization allows the use of different norms to measure perturbation magnitude, and the choice of a norm is a central consideration for nonnormal systems (North 1984; Farrell 1989). The free-

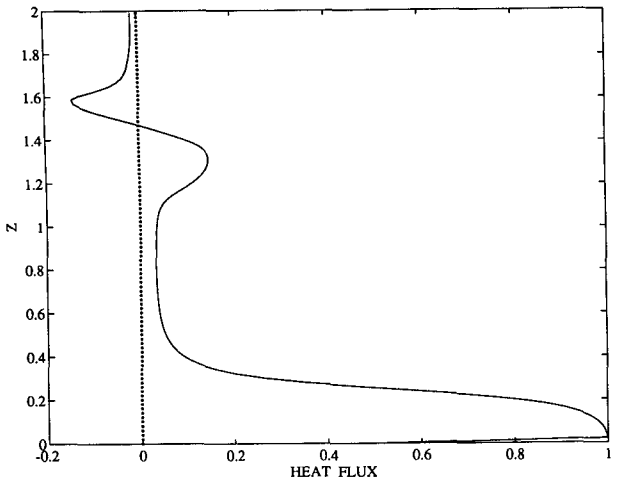

FIG. 6. The distribution of the ensemble average heat flux with height. The basic state is the same as in Fig. 3, $k = 2$, $l = 2$, and $\nu = 10\ m^2\ s^{-1}$.

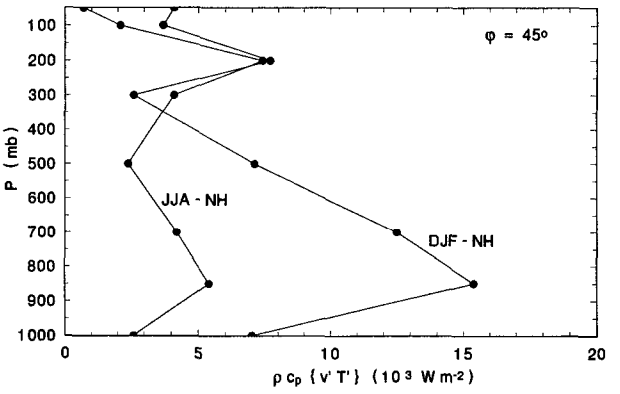

FIG. 7. The distribution of the zonally and seasonally averaged transient heat flux for latitude 45°N, from the values given by Oort and Peixoto (1983). DJF denotes the winter months; JJA denotes the summer months.

dom to choose a norm allows the investigator to concentrate on those aspects of the dynamics that are of greatest interest, perhaps energy growth in one study and, in another context, central pressure fall. This distinction is without consequence in normal dynamic systems.

Among the set of all positive definite quadratic norms associated with the set of nonsingular Hermitian matrices, $\mathcal{M}$, there is the norm of the inner product in which the eigenvectors of $\mathcal{A}$ in (3.2) are orthogonal: $\mathcal{M} = (\Phi \mathcal{G} \Phi^\dagger)^{-1}$; where Φ is the matrix of the eigenvectors of $\mathcal{B}$ arranged in columns, and $\mathcal{G}$ is any positive definite diagonal matrix. This is the measure of perturbation magnitude consisting of a weighted sum of the squared amplitudes of the modes that make up the perturbation (the weighting depends inversely on the diagonal elements of $\mathcal{G}$). So generalized, it is the only norm in which the modes are orthogonal (for a proof of this statement, refer to Farrell and Ioannou 1993b). Despite the apparent simplicity gained by the fact that the dynamical system is normal in the generalized coordinates associated with this norm, the sum of squared amplitudes of the modes making up a disturbance has no obvious physical significance such as attaches to perturbation energy or geopotential variance, which are the metrics of the energy and L_2 norms, respectively. In passing, we remark that it has sometimes been suggested that a natural measure of perturbation magnitude would follow from use of the weightings associated with pseudoenergy or pseudomomentum because the generalized inviscid modes are orthogonal in these inner products (Held 1985). However, even leaving aside the unphysical requirement that the flow be inviscid for their validity, the associated inner products do not in general generate a norm because they have a null space that is spanned by the normal modes.

Finally, we remark that there is a close correspondence between the methods used in this work to obtain the correlation matrix using the given dynamical system and the related data analysis problem of using the observed correlation matrix to obtain the dynamical system and its forcings (Penland 1989).

6. Conclusions

We have examined the mechanism by which a nonnormal system such as the baroclinic atmosphere, that is subject to stochastic forcing can maintain a high level of variance as an amplifier of nonmodal perturbations. The forcing functions (FOFs) ordered in their contribution to the variance are identified with the solution of a particular Lyapunov equation, and the response functions (EOFs) are

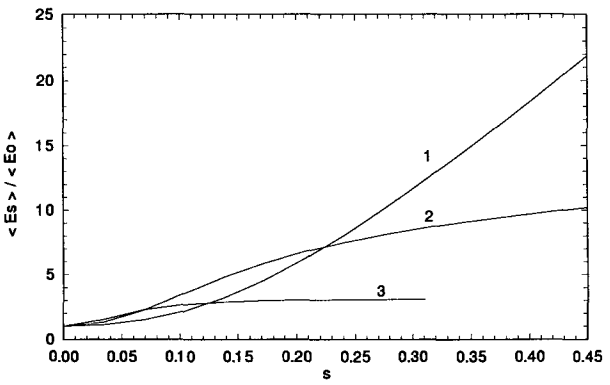

FIG. 8. Variation of ensemble average energy as a function of shear s for different forcing distributions. The variance has been normalized to the value maintained at zero shear $\langle E_0 \rangle$. Curve 1 corresponds to a forcing distribution with a minimum resolved scale of 0.5 km, curve 2 to a forcing distribution with a minimum resolved scale of 1.5 km, and curve 3 to a forcing with a minimum resolved scale of 3.25 km. The case $k = 2$, $l = 2$ is shown, with $\nu = 10\ m^2\ s^{-1}$, and $R = 0.01$.

identified with the solution of a related Lyapunov equation. The primary forcing functions, the primary response functions, and the normal modes are found to be mutually distinct for nonnormal systems such as the baroclinic atmosphere, although these are identical to the normal modes in the case of normal systems. In the atmosphere these forcing functions could arise as projections from diabatic processes that produce potential enstrophy both in the interior through latent heat release and at the boundary from surface heating; in addition, frictional processes operating in strongly sheared frontal regions could introduce potential enstrophy projecting on the primary forcing functions, as could large- and small-scale topographic forcing. But it is possible as well to generalize the notion of a flow operating predominantly as an amplifier to include self-excitation from feedback, just as an acoustic amplifier is well known to break into oscillation when the amplified signal is allowed to sufficiently influence the input. The clear association of latent heat release with cyclones is perhaps the most obvious candidate for closing the atmospheric amplifier feedback loop, although the nonlinear interactions among perturbations are also involved in maintaining dynamically the population of energetically active perturbations.

Regardless of the source of excitation, the linear growth mechanism is solely responsible for transferring energy from the mean flow to the perturbations. In this work the mechanism by which variance is maintained was examined using stochastic forcing to model the source of excitation that induces the transfer of mean flow energy to the perturbation field.

Acknowledgments. Brian Farrell was supported by DOE through the Northeast Regional Center of NIGEC, by NSF ATM-92-16813, and by NASA through University of Maryland 26929A. Petros J. Ioannou was supported by NSF ATM-92-16189.

REFERENCES

Bell, M. J., and A. A. White, 1988: Spurious stability and instability in N-level quasi-geostrophic models. *J. Atmos. Sci.*, **45**, 1731–1738.

Boyd, J. P., 1983: The continuous spectrum of linear Couette flow with the beta effect. *J. Atmos. Sci.*, **40**, 2304–2308.

Charney, J. G., 1947: The dynamics of long waves in a baroclinic westerly current. *J. Meteor.*, **4**, 135–162.

Craik, A. D., and W. O. Criminale, 1986: Evolution of wavelike disturbances in shear flows: A class of exact solutions of the Navier–Stokes equations. *Proc. Roy. Soc. London*, **A-406**, 13–26.

Drazin, P. G., and W. H. Reid, 1981: *Hydrodynamic Stability.* Cambridge University Press, 525 pp.

Farrell, B. F., 1982: The initial growth of disturbances in a baroclinic flow. *J. Atmos. Sci.*, **39**, 1663–1686.

——, 1984: Modal and nonmodal baroclinic waves. *J. Atmos. Sci.*, **41**, 668–673.

——, 1985: Transient growth of damped baroclinic waves. *J. Atmos. Sci.*, **42**, 2718–2727.

——, 1988: Optimal excitation of neutral Rossby waves. *J. Atmos. Sci.*, **45**, 163–172.

——, 1989a: Unstable baroclinic modes damped by Ekman dissipation. *J. Atmos. Sci.*, **46**, 397–401.

——, 1989b: Optimal excitation of baroclinic waves. *J. Atmos. Sci.*, **46**, 1193–1206.

——, 1990: Small error dynamics and the predictability of atmospheric flows. *J. Atmos. Sci.*, **47**, 2409–2416.

——, and P. J. Ioannou, 1993a: Stochastic forcing of perturbation variance in unbounded shear and deformation flows. *J. Atmos. Sci.*, **50**, 200–211.

——, and ——, 1993b: Stochastic forcing of the Navier–Stokes equations. *Phys. Fluids A*, in press.

Gill, A. E., 1982: *Atmosphere-Ocean Dynamics.* Academic Press, 662 pp.

Green, J. S. A., 1960: A problem in baroclinic stability. *Quart. J. Roy. Meteor. Soc.*, **86**, 237–251.

Haidvogel, D. B., and I. M. Held, 1980: Homogeneous quasigeostrophic turbulence driven by a uniform temperature gradient. *J. Atmos. Sci.*, **37**, 2644–2660.

Held, I. H., 1985: Pseudomomentum and the orthogonality of modes in shear flows. *J. Atmos. Sci.*, **42**, 2280–2288.

Hunt, J. C. R., D. J. Carruthers, and J. C. H. Fung, 1991: Rapid distortion theory as a means of exploring the structure of turbulence. *New Perspectives in Turbulence*, L. Sirovich, Ed., Springer-Verlag, 55–103.

Ioannou, P. J., 1992: Stochastic forcing of boundary layer turbulence. *Geophysical Fluids Dynamics Summer Program*, WHOI-93-24, 252–270.

James, I. N., 1987: Suppression of baroclinic instability in horizontal shear flows. *J. Atmos. Sci.*, **44**, 3710–3720.

Joseph, D. D., 1976: *Stability of Fluid Motions I.* Springer-Verlag, 282 pp.

Lefschetz, S., 1963: *Differential Equations: Geometric Theory.* Interscience Publishers, 390 pp.

Lin, S.-J., and R. T. Pierrehumbert, 1988: Does Ekman friction suppress baroclinic instability?, *J. Atmos. Sci.*, **45**, 2920–2933.

——, and ——, 1993: Is the midlatitude zonal flow absolutely unstable? *J. Atmos. Sci.*, **50**, 505–517.

Lindzen, R. S., 1990: *Dynamics in Atmospheric Physics.* Cambridge University Press, 310 pp.

——, 1993: Baroclinic neutrality and the tropopause. *J. Atmos. Sci.*, **50**, 1148–1151.

——, and B. F. Farrell, 1980: The role of polar regions in global climate, and a new parameterization of global heat transport. *Mon. Wea. Rev.*, **108**, 2064–2079.

Lorenz, E. N., 1956: Empirical orthogonal functions and statistical weather prediction. Rep. 1, Statist. Forecasting Project, MIT, 49 pp.

Moffat, H. K., 1967: The interaction of turbulence with strong shear. *Atmospheric Turbulence and Radio Wave Propagation*, A. M. Yaglom and V. I. Tatarsky, Eds., Nauka, 139–154.

Nordeng, T. E., 1990: A model-based diagnostic study of the development and maintenance mechanism of two polar lows. *Tellus*, **42A**, 92–108.

North, G. R., 1984: Empirical orthogonal functions and normal modes. *J. Atmos. Sci.*, **41**, 879–887.

Oort, A. H., and J. P. Peixoto, 1983: Global angular momentum and energy balance requirements from observations. *Advances in Geophysics*, Vol. 25, Academic Press, 355–490.

Orr, W. M'F., 1907: The stability or instability of the steady motions of a perfect liquid and of a viscous liquid. *Proc. Roy. Irish Acad.*, **A-27**, 9–138.

Orszag, S. A., 1971: Accurate solution of the Orr–Sommerfeld stability equation. *J. Fluid Mech.*, **50**, 689.

Penland, C., 1989: Random forcing and forecasting using principal oscillation pattern analysis. *Mon. Wea. Rev.*, **117**, 2165–2185.

Pierrehumbert, R. T., 1984: Local and global baroclinic instability of zonally varying flow. *J. Atmos. Sci.*, **41**, 2141–2162.

Salmon, R., 1980: Baroclinic instability and geostrophic turbulence. *Geophys. Astrophys. Fluid Dyn.*, **15**, 167–211.

Sanders, F., 1986: Explosive cyclogenesis in the West-Central North Atlantic Ocean, 1981–84. Part I: Composite structure and mean behavior. *Mon. Wea. Rev.*, **114**, 1781–1794.

Stone, P. H., 1978: Baroclinic adjustment. *J. Atmos. Sci.*, **35**, 561–571.

Townsend, A. A., 1976: *The Structure of Turbulent Shear Flow.* Cambridge University Press, 429 pp.

Tung, K.-K., 1983: Initial-value problems for Rossby waves in a shear flow with critical level. *J. Fluid Mech.*, **133**, 443–469.

Vallis, G. N., 1988: Numerical studies of eddy transport properties in eddy resolving and parameterized models. *Quart. J. Roy. Meteor. Soc.*, **114**, 183–204.

Wang, M. C., and G. E. Uhlenbeck, 1945: On the theory of the Brownian motion II. *Rev. Modern Phys.*, **17**, 323–342.